Journal of Applied Polymer Science

Miscibility behavior of epoxy thermosets loaded with an oligophosphonate

Ionela-Daniela Carja,[1] Diana Serbezeanu,[1] Tachita Vlad-Bubulac,[1] Corneliu Hamciuc,[1] Vicente Forrat Pérez,[2] Maria Dolores Romero Sánchez,[2] Celia Guillem López,[2] Mónica Fuensanta Soriano[2]

[1]"Petru Poni" Institute of Macromolecular Chemistry, Iasi 700487, Romania

[2]Technological Institute of Construction Marble Technical Unit (AIDICO), 03660, Novelda Alicante, Spain

This article is dedicated to the 65th anniversary of "Petru Poni" Institute of Macromolecular Chemistry of Romanian Academy, Iasi, Romania.

Correspondence to: D. Serbezeanu (E-mail: diana.serbezeanu@icmpp.ro)

ABSTRACT: In this study, a commercial epoxy resin was mixed with a phosphorus-containing oligomer and thermally cross-linked using a mixture of two aliphatic amines as curing agents. The miscibility and the influence of the phosphorus-containing oligomer on the characteristics of epoxy thermosets were investigated by scanning electron microscopy (SEM), thermogravimetric analysis, differential scanning calorimetry, and dynamic mechanical analysis. SEM revealed that phosphorus-containing oligomer was well dispersed into the epoxy matrix. Dynamic mechanical analysis indicated an increase in storage modulus as the phosphorus-containing oligomer content loaded into epoxy matrix increased. Thermogravimetric analysis showed that the onset temperature of phosphorus-containing epoxy thermosets and the peak corresponding to the temperature of decomposition decreased compared with the ones corresponding to the neat epoxy system, whereas the char yield increased with the increase in phosphorus content added into the epoxy networks. To better understand the mechanism of action of phosphorus-containing epoxy thermosets, the char residue was investigated by SEM and energy-dispersive X-ray spectroscopy. © 2014 Wiley Periodicals, Inc. J. Appl. Polym. Sci. **2015**, *132*, 41822.

KEYWORDS: morphology; phase behavior; properties and characterization; structure-property relations; thermogravimetric analysis (TGA)

Received 17 September 2014; accepted 1 December 2014

DOI: 10.1002/app.41822

INTRODUCTION

Epoxy resins are widely used in different applications as adhesives, composites, laminates, encapsulates, marine and protective coatings, etc., because of their great versatility, good chemical resistance, outstanding adhesion, low shrinkage, and high-grade insulation properties.[1–6] Nevertheless, epoxy resins have considerable limitations due to their organic nature, leading to a relatively poor fire behavior, which make them unsuitable to meet the very strict requirements of some applications, for example, integrated circuits packaging.[7,8] Different approaches are reported in the literature for improving the flame resistance and thermal stability of epoxy resins. The incorporation of chlorine and/or bromine atoms into epoxy systems has been widely used.[9,10] However, halogen-containing epoxy resins generate highly toxic and/or very corrosive products during combustion; thus, the current research is directed toward the development of halogen-free flame retardants. Among these, organophosphorus compounds are considered one of the most efficient class of flame retardants.[11–15] Therefore, research efforts are underway to develop polymers that contain phosphorus in either the main or side chains. Phosphorus-containing polymers promote the formation of high amount of char when burning. Furthermore, the quantity of flammable gases is substantially reduced. In some cases, self-extinguishment can occur. The utilization of 9,10-dihydro-9-oxa-10-phosphaphenanthrene-10-oxide (DOPO) or its derivatives has been shown to significantly enhance the flame retardancy of epoxy resins.[11,16,17] Our group has been focused on the design and synthesis of phosphorus-containing monomers and/or polymers, especially derivatives of DOPO, exhibiting excellent flame retardant properties.[18–22] The main advantage of such systems is that the flame retardancy can be improved at concentration lower than 3 wt % phosphorus. Besides this, many other disadvantages such as release of toxic gases upon burning, poor compatibility with epoxy matrix, migration of compounds, etc., can be minimized.

In this study, we describe the preparation and characterization of a commercial epoxy resin loaded with different amounts of a phosphorus-containing oligomer. Scanning electron microscopy (SEM) was used to highlight the good dispersion of phosphorus flame retardant into epoxy matrix. Thermal and mechanical properties were investigated by differential scanning calorimetry (DSC), thermogravimetric analysis (TGA), and dynamic mechanical analysis (DMA).

EXPERIMENTAL

Materials

DOPO was purchased from Chemos GmbH, Germany, and dehydrated before use. Terephthaldicarboxaldehyde and phenylphosphonic dichloride were from Sigma Aldrich and used as received. Diglycidyl ether of bisphenol A (D.E.R. 331, epoxy equivalent weight 182–192 g/equiv) was purchased from DOW Chemical Company. Diethylenetriamine (DETA, active hydrogen equivalent weight 20.6 g/equiv) and isophorone diamine (ISPD, active hydrogen equivalent weight 42.5 g/equiv) were from Sigma Aldrich and used as received.

Measurements

Fourier transform infrared (FTIR) spectroscopy was performed on a Bruker Vertex 70 at frequencies ranging from 4000 to 400 cm^{-1}. Samples were mixed with KBr and pressed into pellets.

^{1}H NMR (400 MHz) spectra were obtained at room temperature on a Bruker Avance DRX spectrometer, using DMSO-d_6 as solvent, and calibrated at 2.512 ppm. The phosphorus content was obtained by molybdenum blue method.[23]

SEM/energy-dispersive X-ray spectroscopy (EDX) was performed on a TESLA BS 301 instrument, at 20 kV. The samples were sputtercoated with a thin layer of gold prior to SEM experiments.

DSC measurements were carried out with a Mettler-Toledo differential scanning calorimeter DSC 12E. The samples (3–5 mg) were heated from room temperature up to 250°C, with a heating rate of 10°C/min under nitrogen atmosphere.

DMA was carried out with a Mettler Toledo DMA861e. Samples of 35 × 10 × 3 mm^3 were used. The test method was performed using the dual cantilever bend mode. The storage modulus (E') and loss modulus (E'') were determined as the solid sample was subjected to temperature scan mode at a ramping rate of 3°C/min from −20°C to 170°C, at a frequency of 1 Hz, strength of 2 N, and a shift of 20 μm.

TGA was performed using a Mettler Toledo TGA/SDTA 851^e balance. Approximately 3–5 mg of sample was heated at 10°C/min from 25°C to 700°C under 20 mL/min nitrogen flow. The TG and their first derivative (DTG) curves were recorded.

Samples of about 15 mg were heated with 10°C/min to 700°C in the thermogravimetric analyzer, cooled to room temperature, and transferred to Bruker Vertex 70 instrument to record the FTIR spectrum of the corresponding pyrolysis residue.

Synthesis of the Monomer and Polymer

1,4-Phenylene-bis((6-oxido-6*H*-dibenz[c,e][1,2]oxaphosphorinyl) carbinol) (**1**) was prepared by nucleophilic addition reaction between DOPO and terephthaldicarboxaldehyde, according to a published procedure.[24] FTIR (KBr, cm^{-1}): 935 (P—O—Ph stretching vibrations), 1203 (P═O stretching vibrations), 1474 (P—Ph aromatic ring in-plane stretching vibrations), 3245 (O—H stretching vibrations). ^{1}H NMR (400 MHz, DMSO-d_6, δ, ppm): 8.33–8.10 (m, 4H), 8.04 (m, 1H), 7.90–7.48 (m, 2H), 7.62 (m, 1H), 7.53–7.11 (m, 12H), 6.45–6.25 (m, 2H), 5.45–5.10 (m, 2H).

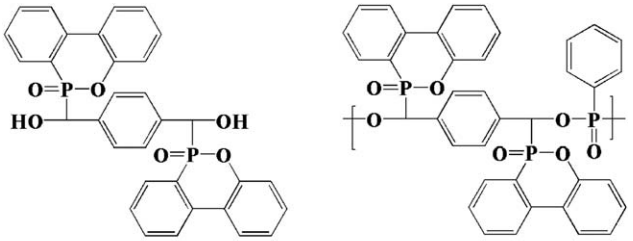

1 **FR**

Figure 1. Chemical structures of monomer (**1**) and oligophosphonate (**FR**) used in this study.

The oligophosphonate (**FR**) was obtained by solution polycondensation reaction of equimolecular amounts of 1,4-phenylene-bis((6-oxido-6*H*-dibenz[c,e][1,2]oxaphosphorinyl)carbinol) (**1**) with phenylphosphonic dichloride.[25] Yield: 91%. FTIR (KBr, cm^{-1}): 931 (P—O—Ph stretching vibrations), 1044 (P—O—C stretching vibrations), 1205 (P═O stretching vibration), 1477 (P—Ph aromatic ring in-plane stretching vibration), 2924 (C—H stretching vibrations). ^{1}H NMR (400 MHz, DMSO-d_6, δ, ppm): 8.46–8.11 (m, 4H), 8.11–8.00 (m, 2H), 8.00–7.79 (m, 4H), 7.79–7.26 (m, 10H), 7.26–7.00 (m, 5H), 5.97–5.19 (m, 2H).

The chemical structure of diol **1** and oligophosphonate **FR** are given in Figure 1.

Preparation of the Phosphorus-Containing Epoxy Thermosets (EP SIPNs)

The phosphorus-containing epoxy thermosets (having a phosphorus content of 2 or 3 wt %) based on a commercial epoxy resin (D.E.R. 331) and oligophosphonate **FR** were prepared by thermal cross-linking in the presence of DETA/ISPD mixture, as curing agents. D.E.R. 331 and the appropriate amount of **FR** were mixed under continuous stirring at room temperature. Afterward, a 1 : 1 molar ratio of DETA/ISPD was added into the mixture, keeping an epoxy to amine equivalent ratio of 1 : 1. The homogeneous reaction mixture was poured into Teflon molds, degassed in a vacuum oven, and then cured at 120°C for 2 h and postcured at 150°C for another 2 h. After the completion of thermal curing reaction, the samples were slowly cooled to room temperature to prevent cracking. The formulations of phosphorus-containing epoxy thermosets (**EP** SIPNs) are listed in Table I.

RESULTS AND DISCUSSION

This work describes the preparation of semi-interpenetrating polymer networks (SIPNs) based on a bisphenol-A type epoxy resin and a oligophosphonate with high content of phosphorus, using a mixture of amines, DETA, and ISPD, as cross-linking agents. Herein, our interest was to investigate the miscibility of

Table I. Preparation of Phosphorus-Containing Epoxy Thermosets

	Weight ratio			
Sample code	D.E.R. 331 (g)	DETA (g)	ISPD (g)	FR (g)
FR	0	0	0	100
EP-0	60	6.11	1.08	0
EP-1	60	6.11	1.08	10.42
EP-2	60	6.11	1.08	17.20

D.E.R. 331 with **FR** and the phase structure of the resulting SIPNs.

The structures of the monomer and oligomer used in this study are presented in Figure 1. The phosphorus-containing epoxy thermosets were prepared by simply mixing the appropriate amount of phosphorus-containing additive (**FR**) into the epoxy resin (D.E.R. 331). The further addition of DETA/ISPD, followed by thermal treatment, led to the formation of **EP** SIPNs.

The structures of **FR**, **EP-0**, and **EP** SIPNs were confirmed using FTIR spectroscopy. The FTIR spectra of **FR**, **EP-0**, and **EP** SIPNs are presented in Figure 2. The characteristic absorption bands of neat **EP-0** system were found at 3432 cm^{-1} (O—H stretching vibrations of unassociated bond in water or phenol and N—H stretching vibrations of secondary amine), 2967 and 2920 cm^{-1} (aliphatic C—H asymmetric stretching vibrations), 2853 cm^{-1} (aliphatic C—H symmetric stretching vibrations), 1607 and 1502 cm^{-1} (aromatic C=C stretching vibrations), 1362 cm^{-1} (C—H deformation vibrations of isopropylidene unit), and 1229 and 1045 cm^{-1} (aromatic C—O—C ether asymmetric and symmetric stretching vibrations, respectively). The **EP** SIPNs showed absorption bands at 3405 cm^{-1} (O—H stretching vibrations of unassociated bond in water or phenol and N—H stretching vibrations of secondary amine), 2967 cm^{-1} (aliphatic C—H asymmetric stretching vibrations), 2867 cm^{-1} (aliphatic C—H symmetric stretching vibrations), 1607 and 1512 cm^{-1} (aromatic C=C stretching vibrations), 1474 cm^{-1} (aromatic P—Ph stretching vibrations), 1205 cm^{-1} (aromatic P=O stretching vibrations), 1044 cm^{-1} (aliphatic P—O—C stretching vibrations), 935 cm^{-1} (aromatic P—O—Ph stretching vibrations), 755 cm^{-1} (deformation vibrations caused by the 1,2-disubstituted aromatic DOPO rings), and at 712 cm^{-1} (deformation vibrations of aromatic rings). The presence of all these bands confirmed the successful incorporation of **FR** into epoxy matrix.[24] There were neither shift of absorption maxima nor new bands appeared, which reveals the existence of weak interactions between **FR** and epoxy matrix.

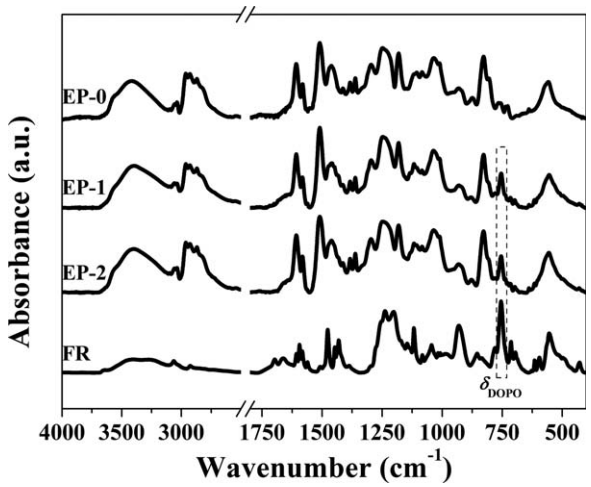

Figure 2. FTIR spectra of **FR**, **EP** SIPNs, and neat **EP-0**.

Figure 3. Photographs of neat **EP-0** system and **EP** SIPNs. [Color figure can be viewed in the online issue, which is available at wileyonlinelibrary.com.]

Figure 3 shows the photographs of neat **EP-0** system and **EP** SIPNs. The **EP** SIPNs were transparent at ambient temperature, and even on further heating up to 150°C, these **EP** SIPNs still presented excellent optical transparency, making them appropriate to be used as protective surface coatings.

SEM was used to observe the morphology of neat **EP-0** system and **EP** SIPNs. The representative SEM photomicrographs of the fracture surfaces are shown in Figure 4. **EP-0** showed a relatively smooth fracture surface with cracks in different planes, indicating the brittle nature of epoxy resin [Figure 4(a)]. In the case of **EP-1** and **EP-2**, the fracture surfaces were full of branches and fibrils disposed almost parallel, suggesting a tough behavior, and high impact strength. Moreover, SEM images of **EP-1** and **EP-2** indicated that **FR** was uniformly dispersed into epoxy matrix and that there were no aggregates, leading thus to a more ductile behavior in the case of **EP** SIPNs [Figure 4(b,c)].

DSC was used to determine the glass-transition temperature of the thermosets and to verify the compatibility between **FR** and epoxy matrix. The T_g values of the oligophosphonate **FR**, neat **EP-0** system, and **EP** SIPNs are given in Table II, and the corresponding DSC curves are shown in Figure 5. Both **EP-1** and **EP-2** SIPNs showed a single T_g value, characteristic for miscible blends. Furthermore, the glass-transition values were higher than the ones corresponding to **FR** and neat **EP-0** system, suggesting that the incorporation of **FR** containing bulky DOPO groups into the epoxy matrix increased the T_g value due to hindered rotation of the polymer chains. Another reason for the increase in T_g values is the fact that incorporation of the source of phosphorous as a oligophosphonate does not imply a nucleophilic attack toward the oxirane rings of the epoxy resin. Subsequently, all the reactive sites are free for the cross-linking process by reaction with the hardeners and overcome the decrease in cross-linking degree as a usual trend when organophosphorus compounds react directly with the oxirane rings.[26]

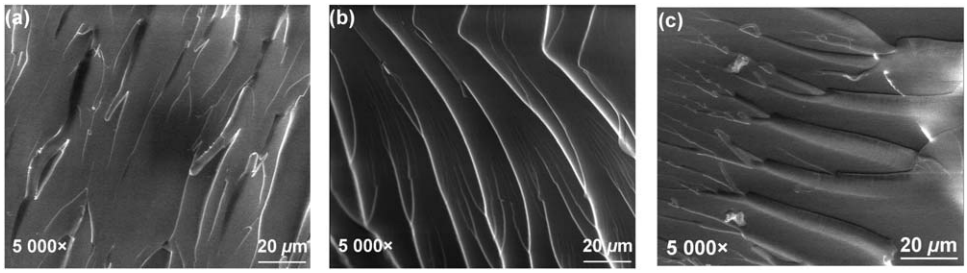

Figure 4. SEM photomicrographs of the cross section of (a) **EP-0**, (b) **EP-1**, and (c) **EP-2**.

Table II. Phosphorus Content and Thermal and Mechanical Characteristics of **FR**, Neat **EP-0** System, and **EP** SIPNs

	Sample code			
	FR	EP-0	EP-1	EP-2
Phosphorus content (P wt %)[a]	13.47	-	2.05	3.09
T_g (°C)	110	125	131	132
E' (GPa)	-	6.82	42.68	27.86
E'' (GPa)	-	0.19	1.13	2.83
T_{onset} (°C)	390	328	289	302
T_{endset} (°C)	495	423	430	429
$T_{max(1,\ 2)}$ (°C)	475	360	344, 440	350, 445
Char yield measured at 700°C (%)	44	7	19	20

[a] The values were experimentally determined.
T_g, glass-transition temperature; E', storage modulus; E'', loss modulus; T_{onset}, onset temperature of polymer decomposition; T_{endset}, endset temperature of polymer decomposition; $T_{max(1,\ 2)}$, thermal decomposition peak corresponding to the temperature of decomposition.

The influence of **FR** added into epoxy matrix was analyzed by DMA, and the main data are listed in Table II. The storage modulus (E') of **EP** SIPNs increased with increasing the amount of **FR**. The storage modulus of **EP-0** at 25°C was 6.82 GPa. When adding 2 wt % phosphorus into epoxy matrix, the storage modulus reached 42.68 GPa. The high storage modulus of **EP-1** SIPN compared with the neat **EP-0** system reveals that **FR** could produce a reinforcing effect by increasing the aromatic density in the network. However, further addition of **FR** did not increase the storage modulus, and even more, it decreased with about 35%. Probably, the high amount of **FR** affected the cross-linked structure between D.E.R. 331 and curing agents. The same behavior was observed in the contribution of Wang *et al.*[8] The increase in loss modulus observed for **EP** SIPNs could be due to the increased energy dissipation in the form of heat as a result of polymer chain movement friction.[24]

Thermal stability of **FR**, **EP-0**, and **EP** SIPNs was evaluated by TGA. The most important data obtained from TG curves are listed in Table II. **FR** is a thermally stable additive used to improve the flame resistance of epoxy resin; it begins to decompose at about 390°C and gives 44 wt % of solid residue at 700°C. The onset degradation temperature of **EP-0** was 328°C, and the char yield measured at 700°C was around 7%. With increasing the **FR** content in epoxy matrix, T_{onset} slightly decreased, probably due to the presence of P—O—C bonds from the **FR** structure, which are more sensitive to thermal degradation.[27] However, with the increase in **FR** content, a higher thermal stability was observed. Accordingly, the char residue increased from 7 to 19 wt % when 2 wt % phosphorus was added into the epoxy matrix (Table II). The high char yield formed during decomposition is correlated with the condensed phase mechanism of phosphorus flame retardants.[28,29] Furthermore, the FTIR spectrum of the char residue at 700°C corresponding to **EP-2** SIPN indicates the presence of phosphorus-containing functional groups (1400 and 1170 cm^{-1}) (Figure 6).[20]

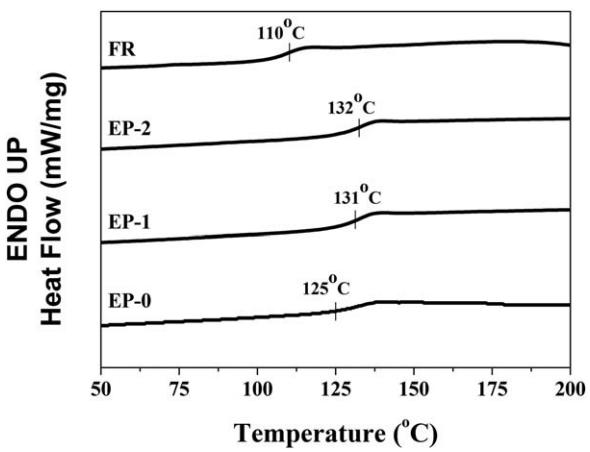

Figure 5. DSC curves of **FR**, **EP-0**, and **EP** SIPN at a heating rate of 10°C/min (second heating).

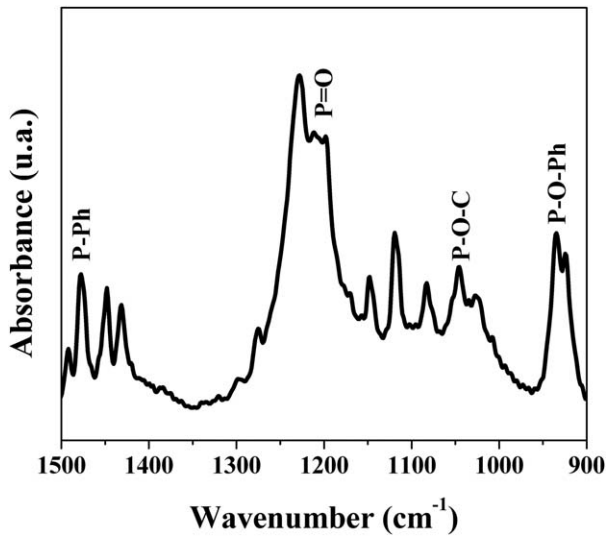

Figure 6. FTIR spectrum of the residual char at 700°C of **EP-2**.

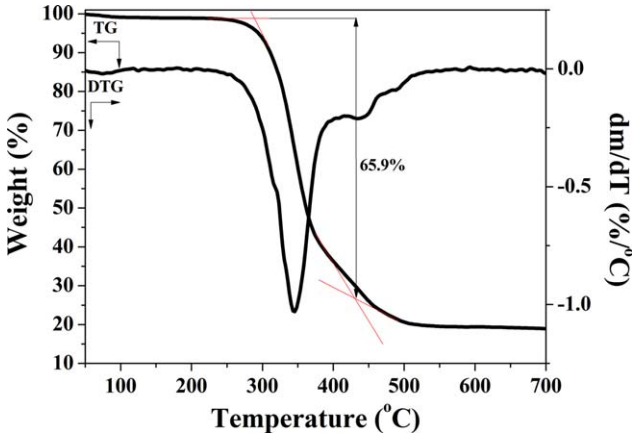

Figure 7. TG and DTG curves of **EP-1** SIPN. [Color figure can be viewed in the online issue, which is available at wileyonlinelibrary.com.]

The TG and DTG curves of **EP-1** SIPN in nitrogen atmosphere are shown in Figure 7. From DTG curves it can be observed that **EP-1** SIPN presents two stages of thermal degradation. The main degradation step took place from 280°C up to 400°C. At temperature above 440°C, the advanced degradation of the carbonaceous residue, formed in the first step, occurred. Sample **EP-2** SIPN followed similar decomposition pathway as that of

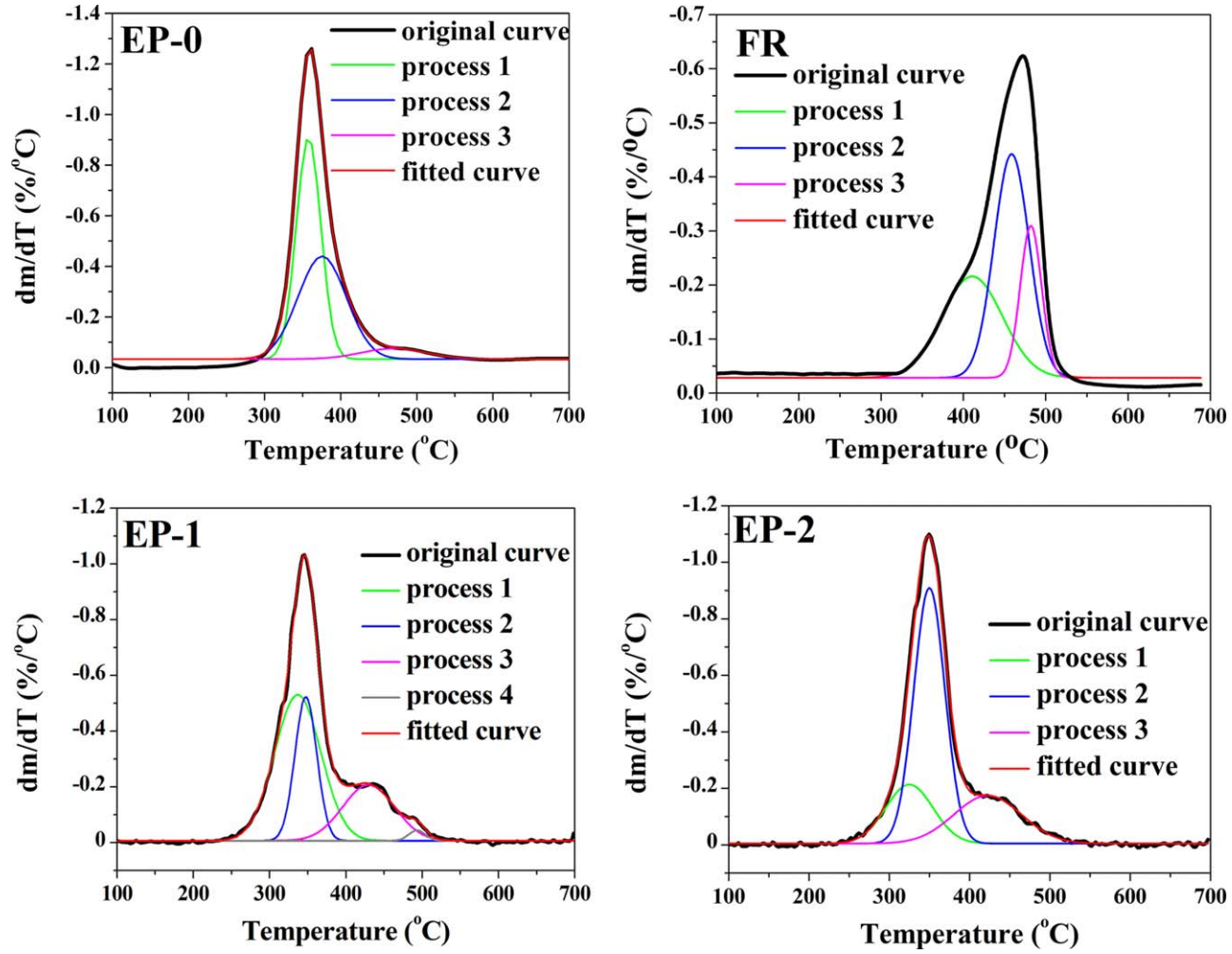

Figure 8. Decomposed DTG curves of **EP-0**, **EP-1**, and **EP-2** SIPNs and **FR**. [Color figure can be viewed in the online issue, which is available at wileyonlinelibrary.com.]

Table III. Decomposition Results of the DTG Curves of **FR**, **EP-0**, and **EP** SIPNs

	Sample code			
	EP-0	EP-1	EP-2	FR
Peak temperature (°C)	358; 376; 470	337; 348; 430; 494	324; 350; 423	409; 459; 482
Peak area (%)	35.41; 32.24; 4.50	40.18; 18.50; 17.22; 1.08	14.92; 44.73; 18.36	17.35; 22.18; 9.24

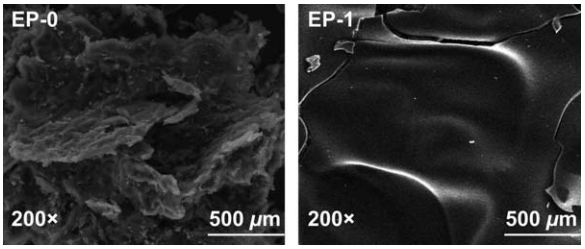

Figure 9. SEM photomicrograph of the char residue at 700°C of **EP-0** and **EP-1** SIPN.

EP-1 SIPN. The sample **EP-2** SIPN presented two maxima of decomposition at 350°C and 445°C and a char yield equal with 20 wt %, measured at 700°C.

Using Gaussian profile, the original DTG curves of **FR**, neat **EP-0** system, and **EP** SIPNs were decomposed in separated curves as shown in Figure 8 (the correlation coefficient $\geq$ 99.9%). This method is useful especially to separate and analyze the overlapping peaks. Table III summarizes the data obtained from DTG curves related with the peak temperature and peak area of the decomposition at different stages during thermal degradation process. The areas of deconvoluted peaks can be correlated with the weight loss (%) values at different stages during thermal degradation. As can be observed, the thermal degradation process of **EP-1** SIPN could be divided in four stages. The number of decomposition stages of **EP-2** SIPN decreased, suggesting a simplification in the complexity of the degradation mechanism. The

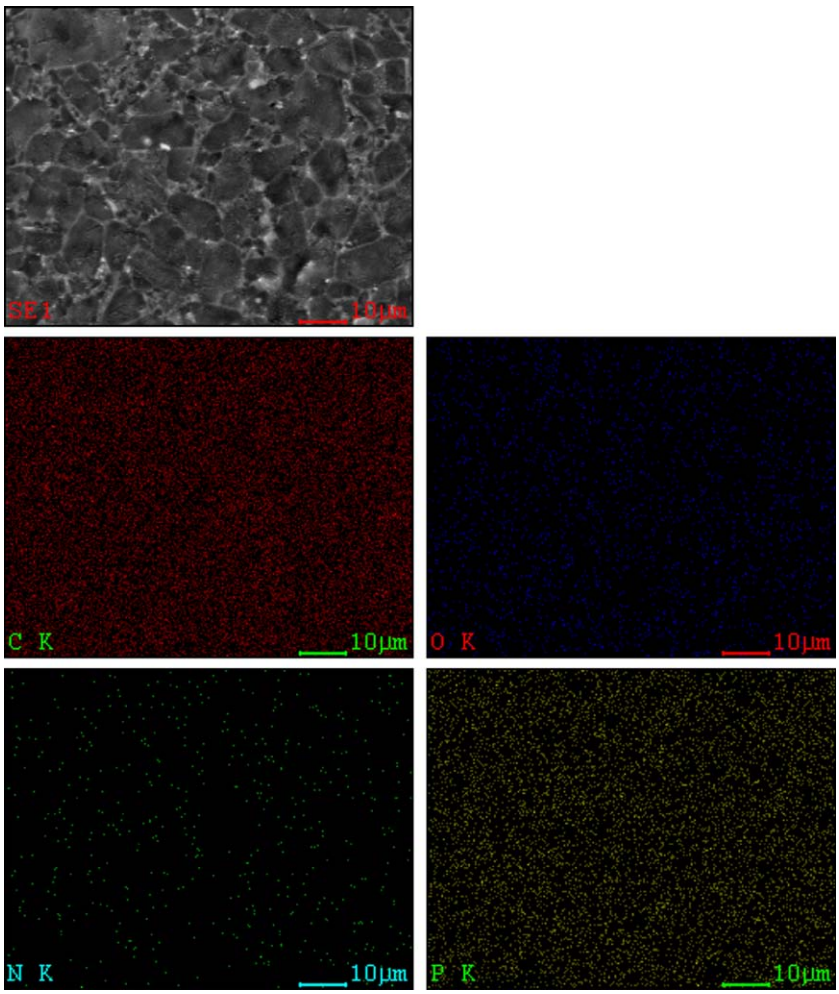

Figure 10. EDX mapping of the char residue of **EP-2** SIPN (SE mode, 20 kV, C: carbon; O: oxygen; N: nitrogen; and P: phosphorus). [Color figure can be viewed in the online issue, which is available at wileyonlinelibrary.com.]

additional degradation process observed in the case of **EP-1** was ascribed to the oxidation of the char residue. By contrast, **EP-2** sample, which contains the highest amount of phosphorus, formed a more thermally stable residual char.

The residual chars obtained after TGA experiments were examined by SEM. Relatively compact and smooth char residues were obtained for both **EP-1** and **EP-2** samples, whereas neat **EP-0** system showed a porous and incompact surface. The formation of compact and continuous char layers is advantageous to induce better flame retardancy in polymeric materials. Figure 9 shows comparatively the char morphology of **EP-0** and **EP-1** SIPN.

In order to investigate the atoms distribution onto the residual char surface, a mapping technique was used. Figure 10 presents the EDX mapping of **EP-2** SIPN. As can be observed, the phosphorus atoms were uniformly dispersed onto the residual char surface.

CONCLUSION

In this study, SIPNs based on a phosphorus-containing oligomer and a commercial epoxy resin were prepared by thermally crosslinking, in the presence of a 1 : 1 molar ratio of DETA/ISPD. The morphological analysis of **EP** SIPNs revealed a good compatibility between epoxy matrix and **FR**. The thermal stability of phosphorus-containing thermosets was investigated by TGA, in inert atmosphere. FTIR spectra of the residual chars of **EP** SIPNs revealed the presence of phosphorus-containing functional groups, indicating thus that the incorporation of **FR** into epoxy matrix resulted in the formation of a more thermally stable phosphorus-rich carbonaceous layer. **FR** was found to be miscible with DER 331 as shown by the existence of a single glass-transition temperature. DMA was used to investigate the influence of phosphorus-containing polymers in EP networks. The high storage modulus of **EP** SIPNs compared with the neat epoxy resin revealed that **FR** could produce a reinforcing effect by increasing the aromatic density in the network. Atoms distribution into the char residue of **EP-0** and **EP** SIPNs was investigated by EDX. The phosphorus atoms were uniformly dispersed onto the char surface.

ACKNOWLEDGMENTS

The authors acknowledge the financial support of CNCSIS–UEFISCSU, Project Number PN-II-RU-TE-0123 no. 28/29.04.2013.

REFERENCES

1. Rodriguez-Mella, Y.; López-Morán, T.; López-Quintela, M. A.; Lazzari, M. *Polym. Degrad. Stab.* **2014**, *107*, 277.
2. Sharmin, E.; Ashraf, S. M.; Ahmad, S. S. *Int. J. Biol. Macromol.* **2007**, *40*, 407.
3. Ma, S.; Gibson, I.; Balaji, G.; Hu, Q. J. *J. Mater. Process. Technol.* **2007**, *192–193*, 75.
4. Marouani, S.; Curtil, L.; Hamelin, P. *Composites Part B* **2012**, *43*, 2020.
5. Toldy, A.; Szolnoki, B.; Marosi, G. *Polym. Degrad. Stab.* **2011**, *96*, 371.
6. Fink, J. K. In Reactive Polymers Fundamentals and Applications, 2nd ed.; Fink, J. K., Ed.; William Andrew Publishing: Oxford, UK, **2013**; pp 95–153.
7. Braun, U.; Balabanovich, A. I.; Schartel, B.; Knoll, U.; Artner, J.; Ciesielski, M.; Döring, M.; Perez, P.; Sandler, J. K W.; Altstädt, V.; Hoffmann, T.; Pospiech, D. *Polymer* **2006**, *47*, 8495.
8. Wang, Z.; Wei, P.; Qian, Y.; Liu, J. *Composites Part B* **2014**, *60*, 341.
9. Terakado, O.; Ohhashi, R.; Hirasawa, M. *J. Anal. Appl. Pyrolysis* **2013**, *103*, 216.
10. Luda, M. P.; Balabanovich, A. I.; Zanetti, M.; Guaratto, D. *Polym. Degrad. Stab.* **2007**, *92*, 1088.
11. Wang, X.; Hu, Y.; Song, L.; Xing, W.; Lu, H. *J. Anal. Appl. Pyrolysis* **2011**, *92*, 164.
12. Lin, C. H.; Wang, Y. R.; Feng, Y. R.; Wang, M. W.; Juang, T. Y. *Polymer* **2013**, *54*, 1612.
13. Gu, L.; Chen, G.; Yao, Y. *Polym. Degrad. Stab.* **2014**, *108*, 68.
14. Sun, D.; Yao, Y. *Polym. Degrad. Stab.* **2011**, *96*, 1720.
15. Liu, W.; Wang, Z.; Xiong, L.; Zhao, L. *Polymer* **2010**, *51*, 4776.
16. Zhang, W.; Li, X.; Yang, R. *Polym. Degrad. Stab.* **2011**, *96*, 1821.
17. Perret, B.; Schartel, B.; Stöß, K.; Ciesielski, M.; Diederichs, J.; Döring, M.; Perret, B.; Schartel, B. *Eur. Polym. J.* **2011**, *47*, 1081.
18. Petreus, O.; Vlad-Bubulac, T.; Hamciuc, C. *Eur. Polym. J.* **2005**, *41*, 2663.
19. Hamciuc, C.; Hamciuc, E.; Serbezeanu, D.; Vlad-Bubulac, T.; Cazacu, M. *Polym. Int.* **2011**, *60*, 312.
20. Serbezeanu, D.; Vlad-Bubulac, T.; Hamciuc, C. *Mater. Plast.* **2011**, *48*, 7.
21. Petreus, O.; Avram, E.; Serbezeanu, D. *Polym. Eng. Sci.* **2010**, *50*, 48.
22. Vlad-Bubulac, T.; Serbezeanu, D.; Hamciuc, C.; Petreus, O.; Carja, I.-D.; Lisa, G. *Polym. Eng. Sci.* **2013**, *53*, 1209.
23. Merz, W. *Mikrochim. Acta* **1959**, *47*, 456.
24. Wang, X.; Hu, Y.; Song, L.; Yang, H.; Xing, W.; Lu, H. *Prog. Org. Coat.* **2011**, *71*, 72.
25. Carja, I.; Serbezeanu, D.; Vlad-Bubulac, T.; Hamciuc, C.; Coroaba, A.; Lisa, G.; López, C. G.; Soriano, M. F.; Pérez, V. F.; Sánchez, M. D. R. *J. Mater. Chem. A.* **2014**, *2*, 16230.
26. Schäfer, A.; Seibold, S.; Walter, O.; Döring, M. *Polym. Degrad. Stab.* **2008**, *93*, 557.
27. Patel, M. B.; Patel, R. G.; Patel, V. S. *J. Therm. Anal.* **1989**, *35*, 47.
28. Paul, J.; Svetlana, T.-M. In Fire and Polymers VI: New Advances in Flame Retardant Chemistry and Science; Morgan Alexander, B.; Wilkie Charles, A.; Nelson Gordon, L., Eds.; American Chemical Society: Washington, DC, **2012**; pp 37–50.
29. Morgan Alexander, B.; Wilkie Charles, A.; Nelson Gordon, L., Eds. Fire and Polymers VI: New Advances in Flame Retardant Chemistry and Science; ACS Symposium Series 1118. American Chemical Society: Washington, DC, **2012**.